



ASF Radiometric Terrain Corrected Products

Sentinel-1 Algorithm Theoretical Basis Document

The Alaska Satellite Facility

ABSTRACT

This document provides the theoretical background of the algorithms and processing flows used for the generation of Sentinel-1 terrain corrected products processed at the Alaska Satellite Facility.

Document preparation

The document was prepared with contributions from

Rudi Gens
 Heidi Kristenson
 Tom Logan
 Jeremy Nicoll

Document change log

Revision	Date	Page	Change Description	Reason for change
1.0 Draft	07/01/2014	all	Initial Draft	
1.1	01/15/2015	all	More detailed description of the algorithm	
1.2	06/01/2015	all	Added more detail on the processing flow	
2.0	06/07/2018	all	Updated document to describe Sentinel processing	
2.1	9/26/2018	all	Added DEM posting; fixed file types	
2.2	10/01/2018	all	JBN Review	
2.3	10/05/2018	all	HJK Review; Added gridding section; Updated calibration section	
3.0	07/20/2020	all	Updated for 2020 Standard RTC products	HyP3 Standard Product release through Vertex
3.1	08/05/2020	all	HJK Review; Added pixel as point reference; Added customizable products	

Table of Contents

Document preparation	2
Document change log	2
Document structure	4
Introduction and scope	5
Background	5
SAR images	5
Calibration	5
Digital elevation models	7
Radiometric Terrain Correction	9
Processing flow	12
Co-registration	12
Product spacing and resolution	12
Radiometric terrain correction	13
DEM Gridding	13
Product generation	13
Customizable Products	14
References	15

Document structure

The document is structured as follows:

Chapter 1 introduces the structure and scope of the document.

Chapter 2 provides background information about SAR imagery, Sentinel-1 calibration, and digital elevation models.

Chapter 3 reviews the theoretical background of radiometric terrain correction.

Chapter 4 shows the processing flow for generating terrain corrected Sentinel-1 products. Details are provided about co-registration, the radiometric terrain correction and products generated.

1 Introduction and scope

The side-looking geometry of SAR imagery leads to geometric and radiometric distortions. This causes foreshortening, layover, shadowing, and radiometric variations due to the slope that make any further analysis difficult (Shimada, 2010).

Radiometric terrain correction improves backscatter estimates that can be used as input for applications such as the monitoring of deforestation, land-cover classification, and delineation of wet snow-covered areas (Small, 2011).

This Algorithm Theoretical Basis Document (ATBD) describes the basic algorithms of radiometric terrain correction using the Gamma Remote Sensing software.

The document will not describe the product specification, data format, and product planning. It will not provide any details of the implementation of the algorithms used.

2 Background

2.1 SAR images

The primary data source for generating geometrically and radiometrically corrected data products is the Sentinel-1 imagery acquired during the Sentinel-1 mission (2014-present). The terrain correction products can be generated for all beam modes using either GRD or SLC image formats. Both Sentinel-1A and Sentinel-1B products can be terrain corrected.

2.2 Calibration

The objective of the calibration of SAR data is to provide imagery in which the pixel values can be directly related to the radar backscatter of the scene. It allows for quantitative analysis of the imagery and comparison between images.

In order to derive geophysical parameters from SAR data, Freeman (1992) established calibration requirements. The specification for γ_0 absolute calibration is ± 1 dB with the long-term relative calibration ± 0.5 dB and the short-term relative calibration less than 0.5 dB.

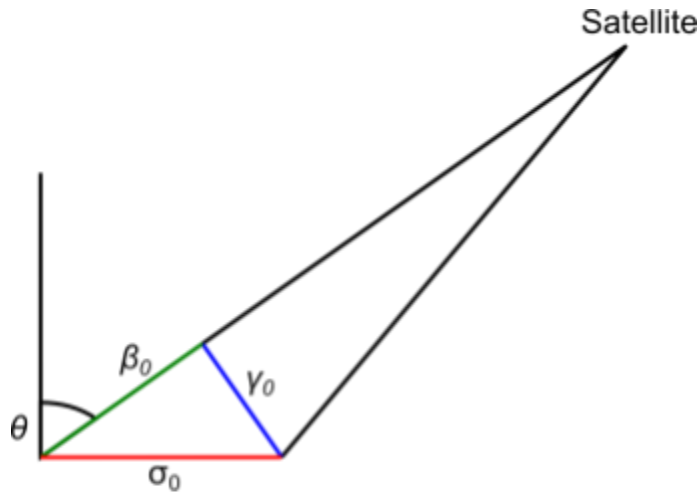


Figure 1: Calibration geometry

Calibrating a SAR image is the process of converting a linear amplitude image into a radiometrically calibrated power image. The input image is in units of digital numbers (DNs), whereas the output image is in units of β_0 , γ_0 , or σ_0 , which is the ratio of the power that comes back from a patch of ground to power sent to the patch of ground (Figure 1).

The application requirements will help determine which of these calibration units to choose. If quantitative measurements referenced to the ground are

required, σ_0 values should be used. For calibration purposes, γ_0 values are preferred because they are equally spaced. Finally, β_0 values are independent from the observed terrain. Values generated in the terrain correction process default to γ_0 . Converting values from γ_0 to σ_0 and β_0 requires the incidence angle θ :

$$\sigma_0 = \gamma_0 \cos \theta, \beta_0 = \frac{\gamma_0}{\tan \theta} \quad (1)$$

Schwerdt *et al.* (2016, 2017) summarized their assessment of the radiometric and geometric calibration of Sentinel-1A and Sentinel-1B data using two types of calibration point targets to determine the calibration factor relating the DNs to normalized a radar cross section (NRCS). Both C-band transponders and trihedral corner reflectors were used to compare actual point target analysis measurements with known radar cross sections.

The NRCS can be calculated using one of three different calibration look up tables producing either β_0 , γ_0 , or σ_0 with the following equation:

$$value(i) = \frac{|DN_i|^2}{A_i^2} \quad (2)$$

The Schwerdt *et al.* analysis determined an absolute radiometric accuracy of 0.43 dB for Sentinel-1A, 0.36 dB for Sentinel-1B, and a cross-check between the systems showed an accuracy of 0.38 dB.

2.3 Digital elevation models

The correction of the geometric distortions as well as the related radiometry adjustment of SAR imagery requires the use of digital elevation models (DEMs). The accuracy of a terrain corrected result is directly related to the quality of the DEM.

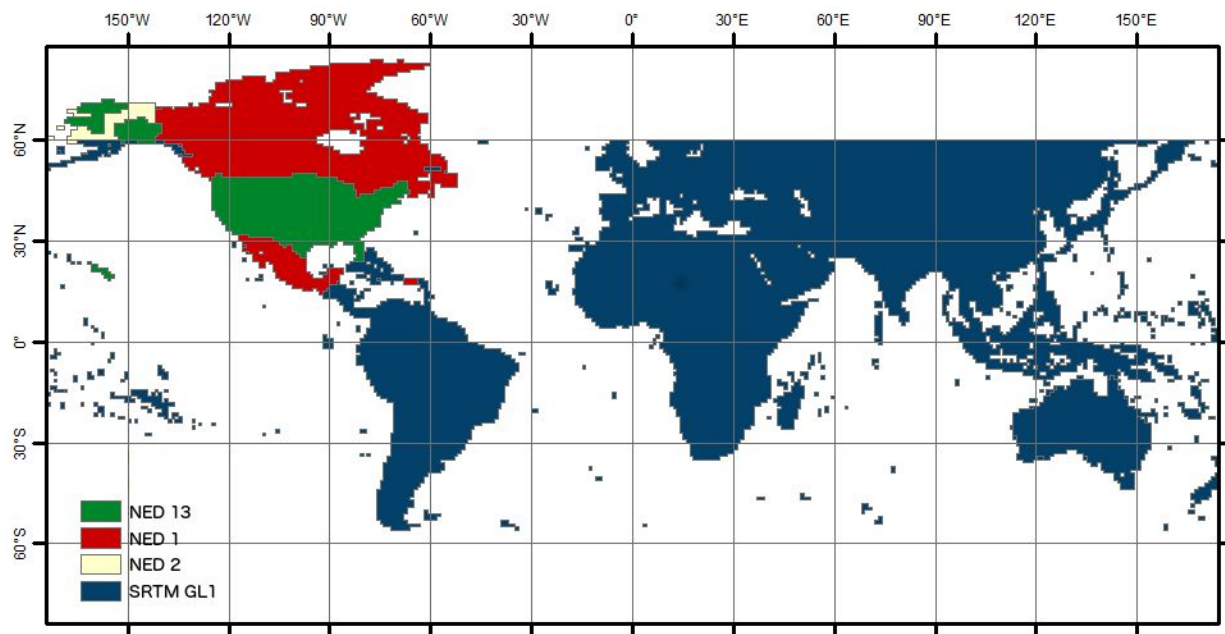


Figure 2: Four different sources of DEMs are used for the terrain correction. Note high resolution DEMs are not available for Greenland, Eurasia above 60 degrees northern latitude, and Antarctica.

Figure 2 shows the coverage of DEMs used for the terrain correction, provided by the United States Geological Survey (USGS). The Shuttle Radar Topography Mission (SRTM) data is globally available at a resolution of 30 m between 60 degrees northern and southern latitude. North America is covered by a variety of digital elevation models. For Canada and Mexico a National Elevation Dataset (NED) at a resolution of 1 arc-second is used. Alaska is generally covered with NED 2 arc-second resolution data as well as SRTM data at 30 m below 60 degrees northern latitude. The USGS provided data for some parts of Alaska and the contiguous United States (CONUS) at a $\frac{1}{3}$ arc-second level.

The SRTM GL1 data showed a number of artifacts that needed to be corrected. In order to detect the anomalies, the slope to the neighboring pixel was calculated in both image directions. Any absolute local slope greater than 400 m was marked as anomaly. The spikes and

holes forming the anomalies in the DEM were removed by adaptive triangulation using the Quick Terrain Modeler software.

The accuracy of these various DEM sources was analyzed by Gesch *et al.* (2014), comparing the DEM with reference data in the form of geodetic control points of the National Geodetic Survey (NGS). The results are summarized in Table 1.

DEM Source	RMSE [m]
CONUS ½ arc-second	1.55
CONUS 1 arc-second	2.44
Alaska 2 arc-second	4.85
Canada 1 arc-second	3.64
Mexico 1 arc-second	6.74

Table 1: Absolute vertical accuracy of the various NED sources (Gesch *et al.*, 2014)

The comparison of 1 arc-second NED with other large-area elevation datasets showed the following accuracies (Table 2):

DEM Source	RMSE [m]
NED 1 arc-second	1.84
SRTM 30 m	4.01
ASTER GDEM 30 m	8.68

Table 2: Accuracy assessment of large-area elevation datasets (Gesch *et al.*, 2014)

The DEMs are organized and assembled as virtual raster mosaics from which the necessary subsets are extracted that cover the relevant areas for the terrain correction. The DEM values are geoid corrected. When DEMs are extracted for scenes to be processed, they are created at a 30-meter posting. Thus they all line up on the same grid automatically.

3 Radiometric Terrain Correction

Radiometric terrain correction addresses two aspects of adjusting the effects of side-looking geometry of SAR imagery. First, the geometric distortions are corrected by using a digital elevation model. Second, the brightness, or radiometry, is adjusted in the affected foreshortening and layover regions.

Small (2011) comprehensively reviewed the various techniques for radiometric terrain correction and concluded that the pixel-area integration approach is the most robust technique available to radiometrically normalize SAR imagery.

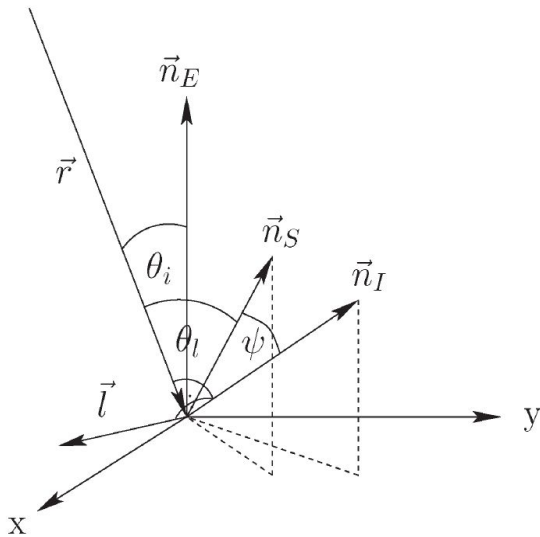


Figure 3: Geometric relationships for angle-based simulations of illuminated area
(Source: Frey *et al.*, 2013)

Figure 3 (Frey *et al.*, 2013) provides the geometric definitions for the illuminated area. \vec{r} is the range vector in the line of sight. \vec{l} is pointing in the azimuth direction. \vec{n}_E is the ellipsoid normal vector. \vec{n}_I is the vector normal to the image plane, the normalized cross product of \vec{l} and \vec{r} . \vec{n}_S is the normalized surface normal vector. θ_i is the ellipsoid-based incidence angle. θ_l is the local incidence angle. Finally, ψ is the projection angle that relates the unit image area to the unit ground area when using the projection cosine approach.

The pixel-area integration for the radiometric normalization adjusts the brightness of the individual SAR image pixels, particularly in layover regions, by determining the actual area on the ground that the SAR signal was backscattered from. The average backscatter coefficient σ_0 is calculated by

$$\sigma_0 = \beta_0 \frac{A_{\sigma_{cos}}^0}{A_{\sigma_{pa}}^0}, \quad (3)$$

using the radar brightness β_0 , the ellipsoid reference area $A_{\sigma_{cos}}^0$, and the illuminated topographic pixel area $A_{\sigma_{pa}}^0$ (Frey *et al.*, 2013).

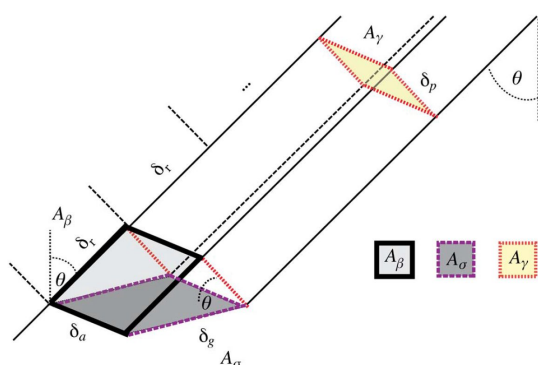


Figure 4: Normalization areas for SAR backscatter (Source: Small, 2011)

The radar brightness β_0 is the ratio of the radar backscatter β and the reference area A_β (Small, 2011).

For a better approximation of the area integral, the digital elevation model is divided into rectangular regions that are then subdivided into two triangular facets (Figure 5). The surface normal is defined for these triangular facets. Based on the geometry relative to the radar look vector (Figure 6), the projected pixel area of the facet is determined and added to the pixel-area map in range-Doppler coordinates.

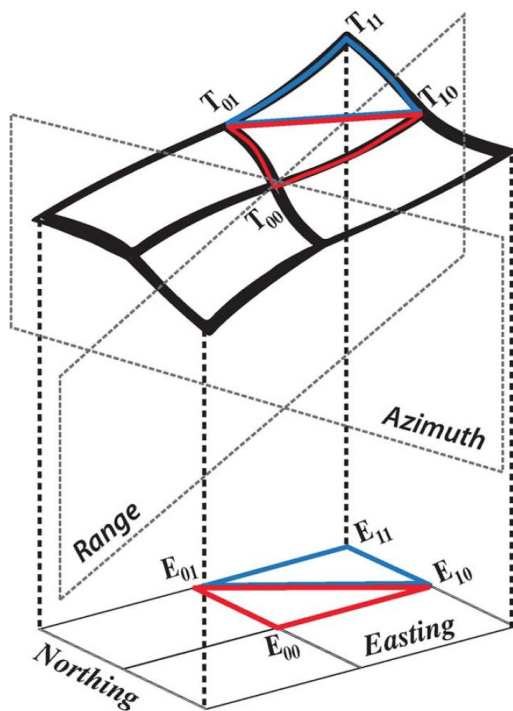


Figure 5: Digital height model facet neighborhood (Source: Small, 2011)

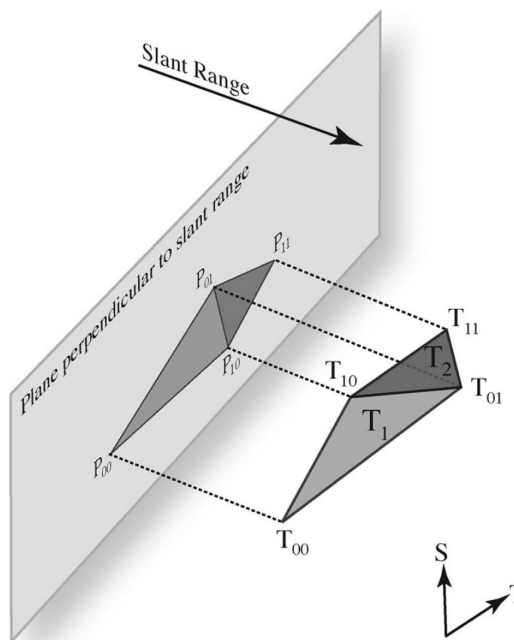


Figure 6: Projection of digital elevation facets into viewing plane (Source: Small, 2011)

In Gamma's implementation of this approach, summarized in Figure 7, each triangular facet is further divided into a number of rectangles that are then integrated into the correct range bin using the same surface normal defined for the triangle.

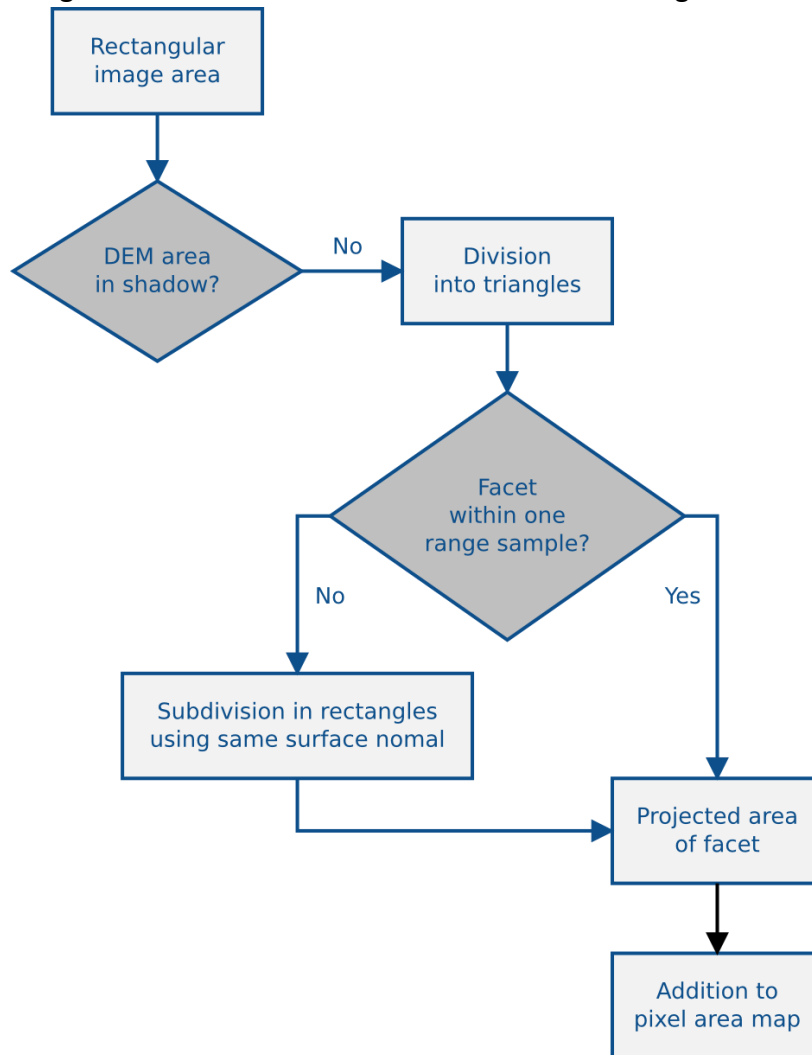


Figure 7: Processing flow for area integration calculation

4 Processing flow

The terrain corrected products are derived from either Sentinel-1 Single Look Complex (SLC) or Ground Range Detected (GRD) products generated by the Sentinel-1 Instrument Processing Facility (IPF).

4.1 Co-registration

In the past, the geolocation quality of the terrain corrected products depended largely on matching the SAR image with a simulated image derived from the DEM during a co-registration process included in the SAR-Simulation Terrain Correction Algorithm (Bayanudin, 2016). This was due to the inaccuracy of the state vectors provided with earlier products.

For the Sentinel platforms, the location of the satellite can be determined to within a few centimeters using a Range-Doppler terrain correction method. Thus, by using the geometric relationship of the satellite and the earth, the imaging swath location is known to a similar accuracy. This approach, also called dead reckoning, relies entirely on the quality of the orbit information provided with the products. By default, no co-registration is used to create the ASF Sentinel-1 RTC images, although there is still the option to use DEM matching for custom-ordered HyP3 imagery, if desired.

4.2 Product spacing and resolution

In order to create a product with a requested pixel spacing, multi-looking is used. Multi-look images are generated by averaging over range and/or azimuth pixels. The process removes speckle, but degrades spatial resolution. The resulting images will have less noise and approximately square pixel spacing. Moreover, after multi-looking, the data will be at the requested pixel spacing after being converted from slant range to ground range.

For the generation of the 30-m RTC products created from GRD inputs, SAR the image is first multi-looked 6x6 to produce an intermediate product that is 60 meters in posting and resolution. This image is then terrain corrected onto a 30 meter grid in the DEM output space, resulting in products that have a resolution of 60 meters and a grid spacing of 30 meters. For 10-m RTC products created from ground range detected inputs, no additional multi-looking is performed. Both product resolution and spacing are preserved (20 meters and 10 meters respectively).

For RTC products derived from SLC inputs, the data is multi-looked 15x3 giving a product that also has roughly 60-meter resolution, and then terrain corrected onto a 30 meter grid. For

10-m RTC products derived from SLC inputs, the data is multi-looked 5x1 giving a product that has roughly 20-meter resolution, and then terrain corrected onto a 10 meter grid.

4.3 Radiometric terrain correction

The adjustment of the radar brightness β^0 is determined by multiplying it by the ratio of pixel area from the ellipsoidal reference A_β over the integrated pixel area A_γ

$$\gamma_T^0 = \beta^0 \cdot \frac{A_\beta}{\int_{DHM} A_\gamma} \quad (4)$$

A side product of the illuminated topographic pixel area calculation is the local incidence angle map.

The inversion of the mapping function used to establish the relation between SAR geometry and the DEM in map-projected space is used to terrain correct and geocode the radiometrically corrected SAR image.

4.4 DEM Gridding

All Sentinel RTC products are placed on the same grid during processing so they will be pixel aligned when created. As a result, no resampling will be required to compare one RTC product to another. This is accomplished by “snapping” the corner coordinates to a regular 30-meter grid that starts at UTM coordinates (0,0). When images are turned into geotiffs, they are written as pixel-as-point data (Open GeotIFF standard 2019).

4.5 Product generation

RTC products will be generated at 30 a meter pixel spacing by default. The layover/shadow mask, incidence angle map and reference DEM included with the product match the pixel spacing of the RTC products.

Standard RTC products are geocoded to the Universal Transverse Mercator (UTM) projection and provided as floating-point values in GeotIFF format. The reference for the RTC products is pixel as point. The products are output in γ_0 radiometric projection in power scale.

4.6 Customizable Products

ASF will release a version of HyP3 that includes the ability to customize products after the initial “standard products” release (slated for fall 2020). Table 3 describes the options that will become available. Product customizations will be reported in the filenames of each product. See the [Sentinel-1 RTC User Guide](#) for the file naming convention.

Parameter	Default	Option	Description
DEM Matching	No matching (Range-Doppler correction)	Matching (SAR-Simulation correction)	DEM matching may be used instead of dead reckoning (default)
Filter	Do not apply a speckle filter	Apply Enhanced Lee speckle filter	Enhanced Lee speckle filter may be applied to remove speckle while preserving edges
Radiometry	γ_0	σ_0	Output product in σ_0 instead of γ_0
Resolution	30m	10m	Output product with 10 meter pixel spacing instead of 30 meter
Scale	Power	Amplitude	Convert power to amplitude by taking the square root of the power values

Table 3: Customizable Options

References

- Bayanudin, A.A. & Jatmiko, R.H., 2016. Orthorectification of Sentinel-1 SAR (Synthetic Aperture Radar) Data in Some Parts Of South-eastern Sulawesi Using Sentinel-1 Toolbox. IOP Conference Series: Earth and Environmental Science, 47, p.012007. Available at: <http://dx.doi.org/10.1088/1755-1315/47/1/012007>.
- Freeman, A., 1992. SAR calibration: an overview. IEEE Transactions on Geoscience and Remote Sensing, 30(6), pp.1107–1121. Available at: <http://dx.doi.org/10.1109/36.193786>.
- Frey, O. et al., 2013. DEM-Based SAR Pixel-Area Estimation for Enhanced Geocoding Refinement and Radiometric Normalization. IEEE Geoscience and Remote Sensing Letters, 10(1), pp.48–52. Available at: <http://dx.doi.org/10.1109/lgrs.2012.2192093>.
- Gesch, D.B., Oimoen, M.J. & Evans, G.A., 2014. Accuracy assessment of the U.S. Geological Survey National Elevation Dataset, and comparison with other large-area elevation datasets: SRTM and ASTER. Open-File Report. Available at: <http://dx.doi.org/10.3133/ofr20141008>.
- Open GeoTIFF Standard 2019, *Raster Space B22*, Open Geospatial Consortium, accessed 4 August 2020, <http://docs.opengeospatial.org/is/19-008r4/19-008r4.html#_raster_space>
- Schwerdt, M. et al., 2014. Independent verification of the Sentinel-1A system calibration. 2014 IEEE Geoscience and Remote Sensing Symposium. Available at: <http://dx.doi.org/10.1109/igarss.2014.6946620>.
- Schwerdt, M. et al., 2017. Independent System Calibration of Sentinel-1B. Remote Sensing, 9(6), p.511. Available at: <http://dx.doi.org/10.3390/rs9060511>.
- Shimada, M., 2010. Ortho-Rectification and Slope Correction of SAR Data Using DEM and Its Accuracy Evaluation. IEEE Journal of Selected Topics in Applied Earth Observations and Remote Sensing, 3(4), pp.657–671. Available at: <http://dx.doi.org/10.1109/jstars.2010.2072984>.
- Small, D., 2011. Flattening Gamma: Radiometric Terrain Correction for SAR Imagery. IEEE Transactions on Geoscience and Remote Sensing, 49(8), pp.3081–3093. Available at: <http://dx.doi.org/10.1109/tgrs.2011.2120616>.